Bull. Mater. Sci., Vol. 35, No. 3, June 2012, pp. 439–447. © Indian Academy of Sciences.

Thermodynamic aspects of nanostructured Ti_5Si_3 formation during mechanical alloying and its characterization

S SABOONI, F KARIMZADEH* and M H ABBASI
Department of Materials Engineering, Isfahan University of Technology, 84156-83111 Isfahan, Iran

MS received 2 April 2011; revised 3 August 2011

Abstract. **Mechanical alloying (MA) was used to produce Ti_5Si_3 intermetallic compound with nanocrystalline structure from elemental powders. The structural changes and characterization of powder particles during milling were studied by X-ray diffraction (XRD), scanning electron microscopy (SEM), transmission electron microscopy (TEM), particle size analyser (PSA) and microhardness measurements. MA resulted in gradual formation of disordered Ti_5Si_3 intermetallic compound with crystallite size of about 15 nm after 45 h of milling. Also a thermodynamic analysis of the process was carried out using Miedema model. The results showed that in the nominal composition of Ti_5Si_3 intermetallic phase ($X_{Si} = 0{\cdot}375$), formation of an intermetallic compound has the lowest Gibbs free energy rather than solid solution or amorphous phases. So the MA product is the most stable phase in nominal composition of Ti_5Si_3. This intermetallic compound exhibits high microhardness value of about 1235 HV.**

Keywords. **Nanostructured materials; Miedema model; characterization; intermetallic compound; Ti_5Si_3.**

1. Introduction

High melting point intermetallic compounds with low density and improved oxidation resistance have been the focus of significant research and development efforts during the last few years. Among the intermetallic compounds, silicides (particularly refractory metal silicides) are well known due to their unique features and good properties (Westbrook and Fleischer 2000). Figure 1 shows the Ti–Si binary phase diagram (Massalski and Okamoto 1990). This equilibrium phase diagram illustrates the existence of four fully stoichiometric silicide phases ($TiSi_2$, TiSi, Ti_5Si_4 and Ti_3Si). The fifth silicide phase, Ti_5Si_3, is the only phase that exhibits a degree of non-stoichiometry. Ti_5Si_3 intermetallic compound is being recognized as a high temperature structural material because of its satisfactory corrosion resistance, low density ($4{\cdot}32$ g/cm^{-3}), high melting point (2130°C) and good wear resistance (Li *et al* 2002; Yeh *et al* 2007; Wang *et al* 2008). However, low ductility at ambient temperature and low strength at elevated temperatures have restricted many of its applications (Kang *et al* 1999). It should be noted that the unsuitable ductility of this compound is related to low symmetry ($D8_8$) in crystal structure and highly covalent bonding that increases the Peierls stress.

Monolithic Ti_5Si_3 has been fabricated by various methods including arc melting of Ti and Si (Zhang and Wu 1998), shock assisted synthesis (Thadhani *et al* 1999) and self propagating combustion synthesis (Riley *et al* 2006). The final product in all of these processes was brittle and had low fracture toughness. It is reported that one way to overcome this problem is nanocrystallization (Enayati *et al* 2008; Mousavi *et al* 2008; Forouzanmehr *et al* 2009). In fact, by decreasing the grain size to nanometric scale, it would be expected that fracture toughness improves. One method for synthesis of nanocrystalline materials is mechanical alloying (MA) (Suryanarayana 2001). Although MA of $Ti_{62{\cdot}5}Si_{37{\cdot}5}$ has been investigated in the literature, but different products have been reported. For example, Yang *et al* (2000) reported an amorphous phase formation while Oehring and Bormann (1991) reported that MA of the powder mixture led to synthesis of Ti_5Si_3 intermetallic compound. Also Oleszak *et al* (1993) reported that during MA of $Ti_{62{\cdot}5}Si_{37{\cdot}5}$ powder mixture, initially an intermetallic compound and then an amorphous phase was formed. From this standpoint, a thermodynamic analysis could help to predict the more stable phase and compare the stability of phases in Ti–Si binary system.

Although MA is a non-equilibrium process and in such a non-equilibrium process, formation of non-thermodynamically unstable phases is possible, but recent research works showed that during mechanical alloying, the first phase formed is always the most thermodynamically stable phase (Guang *et al* 2006; Kesheng *et al* 2007).

In this study, besides the thermodynamic analysis using Miedema model to compare the stability of phases in Ti–Si system, MA of $Ti_{62{\cdot}5}Si_{37{\cdot}5}$ was also investigated more precisely to study nanocrystalline Ti_5Si_3 intermetallic synthesis and the mechanism of Ti_5Si_3 formation during MA. Also the phase transitions, SEM study and microhardness variations during milling were investigated.

*Author for correspondence (karimzadeh_f@cc.iut.ac.ir)

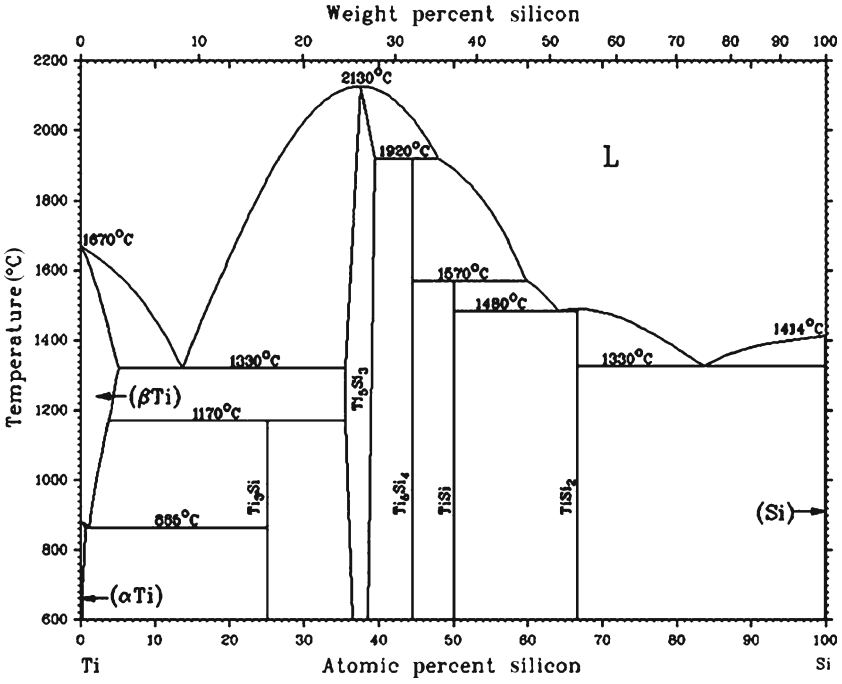

Figure 1. Ti–Si binary phase diagram.

2. Experimental

The powders of Ti and Si were used as starting materials to produce Ti_5Si_3 intermetallic compound. The specifications of raw materials are given in table 1. SEM micrographs of initial powder particles are shown in figure 2. As shown, Si powder particles are angular and Ti powders are irregular in shape.

For the synthesis of Ti_5Si_3 compound, the initial powders were mixed with the stoichiometric ratios and mechanically alloyed in a planetary ball mill at room temperature under argon atmosphere. The experiments were carried out in a hardened chromium steel container with five steel balls. In all MA runs the ball to powder weight ratio and rotational speed were 10:1 and 500 rpm, respectively. Structural changes of powder particles were studied by X-ray diffraction (XRD) in a Philips XPERT MPD diffractometer using CuKα radiation. Williamson–Hall (1953) method was used to determine the crystallite size and internal strain

$$B\cos\theta = \frac{0{\cdot}9\lambda}{D} + 2\varepsilon\sin\theta, \qquad (1)$$

where θ is the Bragg diffraction angle, D the average crystallite size, ε the average internal strain, λ the wavelength of radiation used and B the diffraction peak width at half maximum intensity. In Williamson–Hall method both broadening contributions due to strain and crystallite size are taken into account. A thermodynamic analysis based on Miedema model was also performed to predict the more stable phase and compared with MA results. The morphology and microstructure of mechanically alloyed powders were observed by SEM (in a Philips XL30) and TEM (in a Philips EM208s). The milled powders after 45 h of MA were isothermally annealed at 850 and 1050°C for 60 min under argon atmosphere to study phase transition during annealing. For annealing, the powders were placed inside a capsule and then heat treated under argon atmosphere. After annealing, the capsule was cooled in air. Particle size analyser was used to determine the size distribution of final powder particles. The microhardness of powder particles was determined using a microhardness tester with a Vickers indenter at a load of 50 g and dwell time of 10 s. An average of 5 indentations for each sample were calculated and reported as hardness values.

Table 1. Specification of raw materials.

Elements	Ti	Si
Purity	98+	99+
Particle size	< 150 μm	< 100 μm
Company	Merck	Merck

3. Results and discussion

3.1 *Thermodynamic analysis*

Thermodynamic analysis was carried out to predict the more stable phase and compared with MA results. Crystalline pure elements were chosen as standard states. So the Gibbs

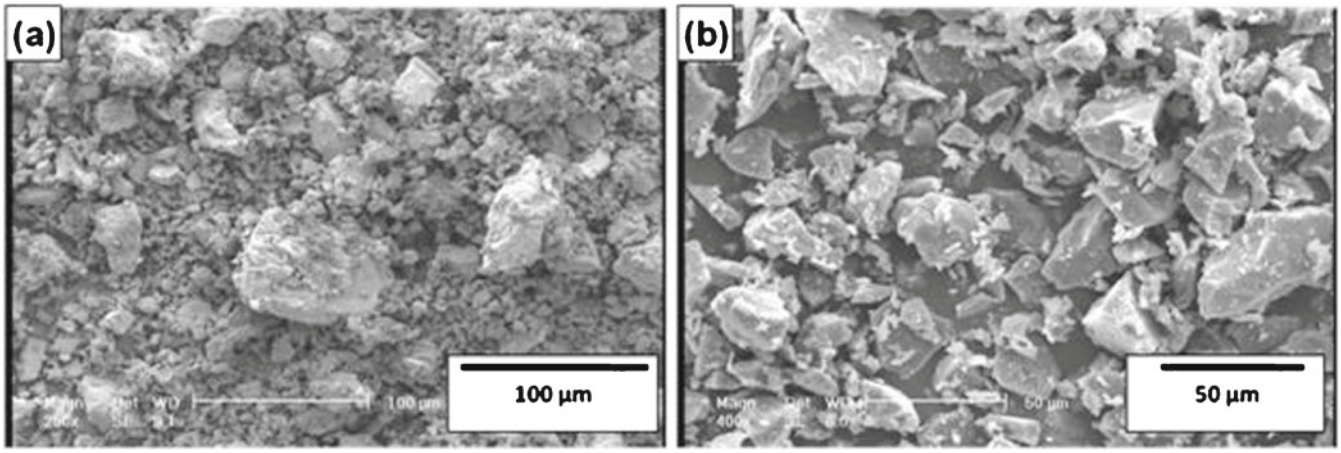

Figure 2. SEM micrographs of initial powder particles: (**a**) pure Ti and (**b**) pure Si.

free energy change for the formation of a solid solution or amorphous phase can be represented as

$$\Delta G = \Delta H - T\Delta S, \tag{2}$$

where ΔH and ΔS are the enthalpy and entropy changes due to mixing, respectively.

According to Miedema's model, the enthalpy of formation of a solid solution consists of three terms (Miedema *et al* 1981; Mousavi *et al* 2009)

$$\Delta H^s = \Delta H_{\text{chemical}} + \Delta H_{\text{elastic}} + \Delta H_{\text{structural}}. \tag{3}$$

The first term on the right hand side of (3) represents the chemical contribution that is due to the electron redistribution that occurs when the alloy is formed. The second term represents the elastic mismatch and the third term represents the lattice stability which is supposed to vary continually with the average number of valence electrons.

According to Miedema and Niessen semi-experimental model

$$\Delta H_{\text{chemical}} = X_A X_B \left(f_B^A \Delta H_S^{A \text{ in } B} + f_A^B \Delta H_S^{B \text{ in } A} \right), \tag{4}$$

where $\Delta H_S^{A \text{ in } B}$ is the solution enthalpy of A in B and is represented as

$$\Delta H_S^{A \text{ in } B} = \frac{V_A^{2/3}}{\left(n_{\text{ws}}^{-1/3}\right)_{\text{av}}} \times \left\{ -P\left(\Delta\Phi^*\right)^2 + Q\left(\Delta n_{\text{ws}}^{\frac{-1}{3}}\right)^2 - R^* \right\}, \tag{5}$$

$$f_B^A = X_B^S \left\{ 1 + \gamma \left(X_A^S X_B^S \right)^2 \right\}, \tag{6}$$

$$X_B^S = \frac{X_B V_B^{2/3}}{X_B V_B^{2/3} + X_A V_A^{2/3}}, \tag{7}$$

where X_A and X_B are molar fractions of elements A and B, Φ^*, V and n_{ws} are work function, molar volume and electron density of the constituents, respectively. P, Q and R^* are constants depending on components. γ is taken to be 0 for solid solution, 5 for amorphous and 8 for intermetallic compounds, respectively.

The elastic contribution of enthalpy ($\Delta H_{\text{elastic}}$) can be expressed as

$$\Delta H_{\text{elastic}} = x_A x_B (x_B \Delta E_{A \text{ in } B} + x_A \Delta E_{B \text{ in } A}), \tag{8}$$

where $\Delta E_{A \text{ in } B}$ and $\Delta E_{B \text{ in } A}$ are the elastic energies caused by A dissolving in B and B dissolving in A, respectively and can be estimated by (9) (Niessen and Miedema 1983)

$$\Delta E_{A \text{ in } B} = \frac{2K_A.G_B(\Delta V)^2}{3K_A.V_B + 4G_B V_A}, \tag{9}$$

$$\Delta E_{B \text{ in } A} = \frac{2K_B.G_A(\Delta V)^2}{3K_B.V_A + 4G_A V_B},$$

where K and G are bulk and shear modulus, respectively.

$\Delta H_{\text{structural}}$ reflects the fact that transition metals show preference to crystallize in one of the three simple crystallographic structures *bcc*, *fcc* and *hcp* depending on the number of valence electrons. This term is only applicable in binary

Table 2. Parameters for thermodynamic calculation at 298 K (Brands 1983; Niessen *et al* 1988; Vander Kolk *et al* 1988).

	T_m (K)	n_{ws} (10^{23} e/cm^3)	φ^* (V)	P (kjV^{-2} cm^{-1})	Q (kjV^{-1})	V (cm^3/mol)	K (GPa)	G (GPa)
Ti	1943	3·18	3·65	12·3	115·6	10·5	137·8	48·3
Si	1687	3·37	4·7	12·3	115·6	8·6	235	40

transition metal systems (Mousavi *et al* 2009). So this term is zero in Ti–Si system.

For an amorphous alloy, both the elastic and structural enthalpies can be neglected (Niessen and Miedema 1983), because there is no crystal structure and the atoms can arrange themselves in such a way that mismatch is avoided (Bakker *et al* 1995). So the enthalpy of amorphous phase formation can be calculated as below (Zhang *et al* 1993):

$$\Delta H_{\text{amorphous}} = \Delta H_{\text{chemical}} + 3{\cdot}5\langle T_{\text{m}}\rangle\,. \tag{10}$$

The second term of this equation reflects the topological disorder in the amorphous state and is estimated by Miedema as 3·5 $\langle T_{\text{m}}\rangle$. Where $\langle T_{\text{m}}\rangle = X_A T_{\text{m}}^A + X_B T_{\text{m}}^B$ and T_{m}^A and T_{m}^B are the melting points of A and B elements, respectively.

For the formation of ideal solid solution from elemental powders, ΔS is calculated with the assumption of configurational entropy change due to mixing:

$$\Delta S^{\text{s}} = -R\,(x_A \ln x_A + x_B \ln x_B)\,, \tag{11}$$

where R is the universal gas constant.

For the formation of an amorphous phase, in addition to the configurational entropy change, an entropy term equal to 3·5 J/mol K should be considered due to the disorder nature of an amorphous phase compared to solid solution. Table 2

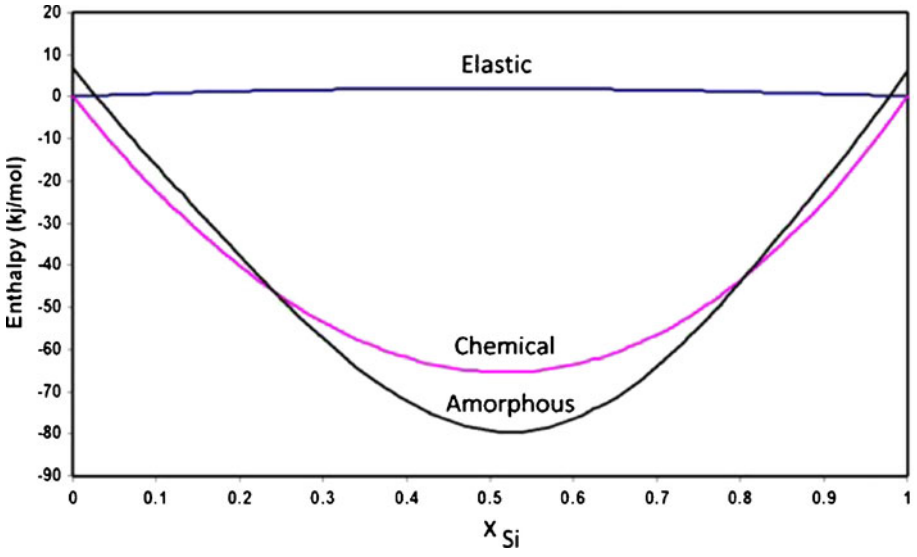

Figure 3. Two contributions to enthalpy change of solid solution and enthalpy change due to amorphous phase formation.

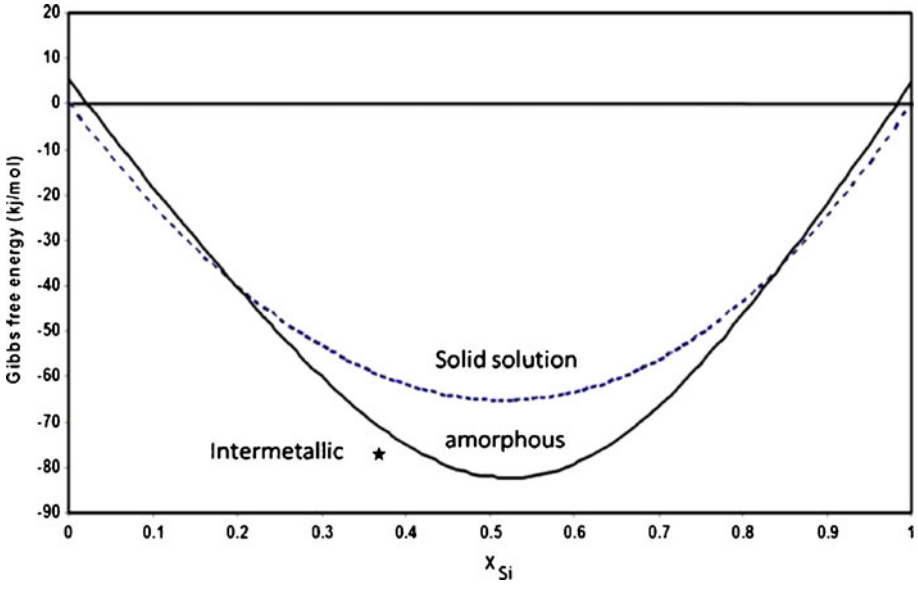

Figure 4. Gibbs free energy changes for formation of solid solution, amorphous and Ti_5Si_3 intermetallic phases in Ti–Si system.

shows required data for calculations of Gibbs free energy change in Ti–Si system.

In figure 3, the two contributions to enthalpy change of solid solution and enthalpy change due to amorphous phase formation, $\Delta H_{\text{amorphous}}$, are shown. It should be mentioned again that $\Delta H_{\text{structural}}$ in the Ti–Si system is zero, because Si is a non-transition metal. As mentioned before, $\Delta H_{\text{elastic}}$ is due to atomic size mismatch. So, as figure 3 shows, this value is small in Ti–Si system at all compositions because of the insignificant difference between atomic radius of Ti and Si. So chemical enthalpy is the major contribution for solid solution formation in Ti–Si system that is due to the difference between bonding energy in initial state and solid solution.

The calculated Gibbs free energy change for the formation of solid solution, amorphous and Ti_5Si_3 intermetallic phase in Ti–Si system are shown in figure 4. The first conclusion derived from figure 4 is that in the composition range of $0{\cdot}0 < X_{Si} < 0{\cdot}02$ and $0{\cdot}98 < X_{Si} < 1$, the Gibbs free energy change for the formation of amorphous phase is positive, that means there is no driving force to form amorphous phase in these composition ranges. In fact, the molar fractions of solutes are very small and cannot have any effect on the crystalline structure of base metal. Figure 4 also indicates that in the composition range between $0{\cdot}2 < X_{Si} < 0{\cdot}85$, the Gibbs free energy change for the formation of amorphous phase is more negative than solid solution. However, for $X_{Si} = 0{\cdot}375$ (nominal composition of Ti_5Si_3 intermetallic phase), the Gibbs free energy change for intermetallic phase is more negative compared to both amorphous and solid solution phases. So the thermodynamic analysis predicts that Ti_5Si_3 intermetallic compound is more stable phase at its nominal composition rather than amorphous or solid solution phases.

3.2 *MA of $Ti_{62{\cdot}5}Si_{37{\cdot}5}$ powder mixture*

3.2a *Structural evolution during MA and subsequent heat treatment*: Figure 5 shows XRD patterns of $Ti_{62{\cdot}5}Si_{37{\cdot}5}$ powder mixture as-received and after different milling times. XRD pattern of as-received powder mixture shows only diffraction peaks of Ti and Si as starting materials. Increasing the milling time to 15 h led only to broadening of XRD peaks and decreasing their intensity and no structural changes were observed. Occurrence of these phenomena is due to the refinement of crystallite size and increase of internal strain of Ti and Si powders (Cullity 1978). After 30 h of MA, in addition to the peaks related to Ti and Si, new peaks related to Ti_5Si_3 began to appear. In fact, after 15 h of MA, the gradual interaction between Ti and Si took place and caused the formation of Ti_5Si_3. Finally it seems that complete transformation of Ti and Si powders to Ti_5Si_3 intermetallic compound occurred after 40 h of MA. The crystallite size and internal strain of Ti_5Si_3 intermetallic compound after 45 h of MA were 15 nm and 1·8%, respectively. These results are listed in table 3.

Depending on MA conditions, two different reaction kinetics are possible (Takacs 2002): (i) Sudden formation of products in a short period of milling time and consequently occurrence of mechanically alloyed self sustaining reaction and (ii) the reaction may extend to a small volume during each collision resulting in a gradual mechanism.

According to the Munir and Anselmi–Tamburini rules, a self sustaining reaction can be initiated without any external source when $\Delta H/C_p \geq 2000$, where ΔH and C_p are the reaction heat and room temperature heat capacity of product, respectively (Lu and Li 2005). It should be noted that this criterion is a simplified form of adiabatic temperature (T_{ad}). The only difference between adiabatic temperature and

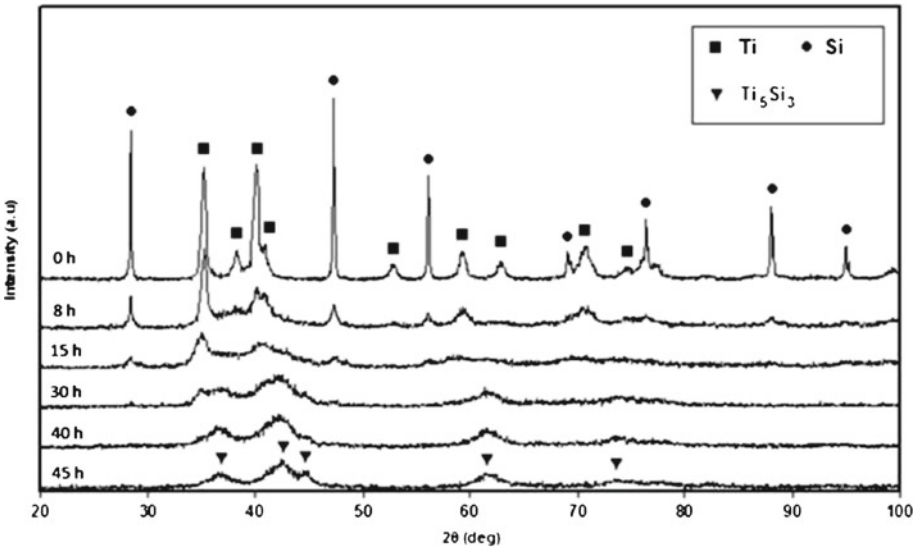

Figure 5. XRD patterns of $Ti_{62{\cdot}5}Si_{37{\cdot}5}$ powder mixture as-received and after different milling times.

Table 3. Characteristic parameters of $Ti_{62.5}Si_{37.5}$ powder mixture after different processes.

Process	Crystallite size (nm)	Lattice strain	LRO	Hardness (HV)
45 h of MA	15	1·8	–	1235
45 h of MA + annealing at 850°C	35	0·75	0·66	1050
45 h of MA + annealing at 1050°C	46	0·6	0·7	1000

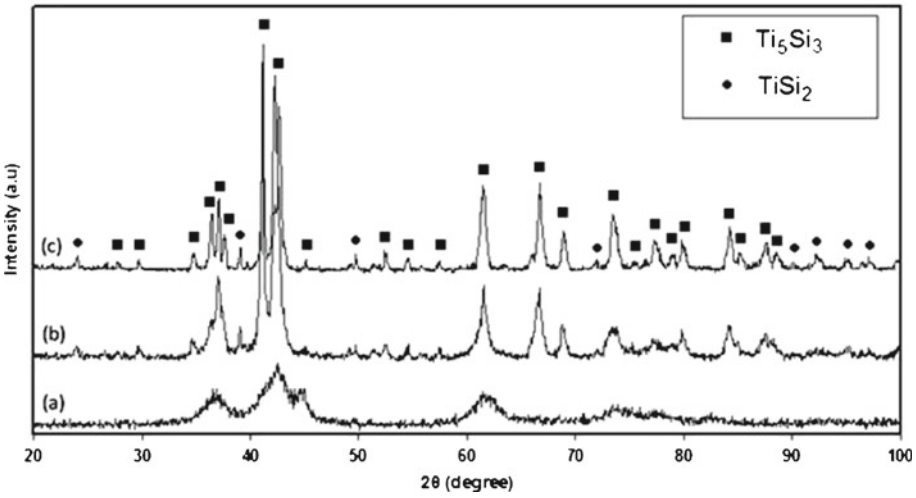

Figure 6. XRD patterns of powder mixture: (**a**) after 45 h of MA, (**b**) after annealing at 850°C for 1 h and (**c**) after annealing at 1050°C for 1 h.

$\Delta H/C_p$ is that the latent heat of melting and evaporation are left out (Takacs 2002). Also it has been suggested empirically that the value of adiabatic temperature should be above 1800 K to yield self propagating combustion reaction in thermally ignited systems. The $\Delta H/C_p$ and T_{ad} criterions for the formation of Ti_5Si_3 from elemental powders were calculated to be about 3100 and 2500 (Doppiu *et al* 2001), respectively which are higher than critical values of 2000 and 1800. But no explosive reaction was observed in our experiments whereas Cheon *et al* (2007) reported that an explosive reaction was observed in the MA of $Ti_{62.5}Si_{37.5}$ powder mixture in a high energy mill. In a planetary ball mill the amount of impact energy given to the particles at each collision is much lower than high energy ball mills. The ignition of mechanically-alloyed self sustaining reaction (MSR) process needs hot spots to initiate this reaction. So impact energy of planetary ball mill is not enough to conduct an explosive reaction in this system. This behaviour was also observed by other investigators in other systems (Lu and Li 2005). So it can be concluded that besides the reaction characteristics, the milling dynamics is also important for the occurrence of gradual or explosive reactions.

With higher focus on the XRD patterns, it can be seen that the position of Ti and Si peaks were not changed during MA. This means that the dissolution of these elements did not occur. So, with respect to the gradual formation of Ti_5Si_3, it can be found that the formation of Ti_5Si_3 phase develops by continuous diffusive reaction at Ti/Si layer interface formed during MA. This mechanism was also observed in other binary systems (Enayati *et al* 2008).

After 45 h of MA, the final product was annealed at 850 and 1050°C for 60 min. Figure 6 shows XRD patterns of 45 h milled and heat-treated samples. After annealing it was observed that the width of fundamental diffraction peaks decreased as compared to the results of milled powders. This is due to the grain growth and decrease of lattice distortion as shown in table 3. Also a small amount of $TiSi_2$ phase was detected in XRD patterns of annealed samples. It was reported that existence of a small amount of this silicon-rich phase can improve high oxidation resistance of Ti_5Si_3 intermetallic compound (Tang *et al* 2008). Another important feature that should be noted is the presence of Ti_5Si_3 superlattice peaks (Rao and Zhou 2004) after annealing at both 850 and 1050°C that indicates an increase in $D8_8$ ordering which occurred during annealing.

In order to quantify the degree of ordering, long range order parameter, S, was determined from the intensities of a superlattice reflection and a fundamental reflection with respect to the homogenized reference material according to the equation given by Bakker *et al* (1995)

$$S = \sqrt{\frac{\left(I_S/I_F\right)_{dis}}{\left(I_S/I_F\right)_h}}, \tag{12}$$

where $(I_S/I_F)_{dis}$ and $(I_S/I_F)_h$ are the intensity of superlattice reflection taken relative to the fundamental line for the disordered (e.g. milled) and homogenized reference (hr) powder, respectively.

It should be noted that intensities of homogenized reference powders can be derived from JCPDS files. Using (12), LRO was obtained as 0·66 and 0·7 after annealing at 850 and 1050°C, respectively. It can be noted that annealing at 1050°C leads to lower density of lattice defects and therefore, more ordering in structure.

3.2b *Morphological and microstructural changes*: Figure 7 shows morphology of mechanically alloyed powders after different milling times. MA for 0·5 h caused only mixing of Ti and Si as starting materials. After 5 h of MA, cold

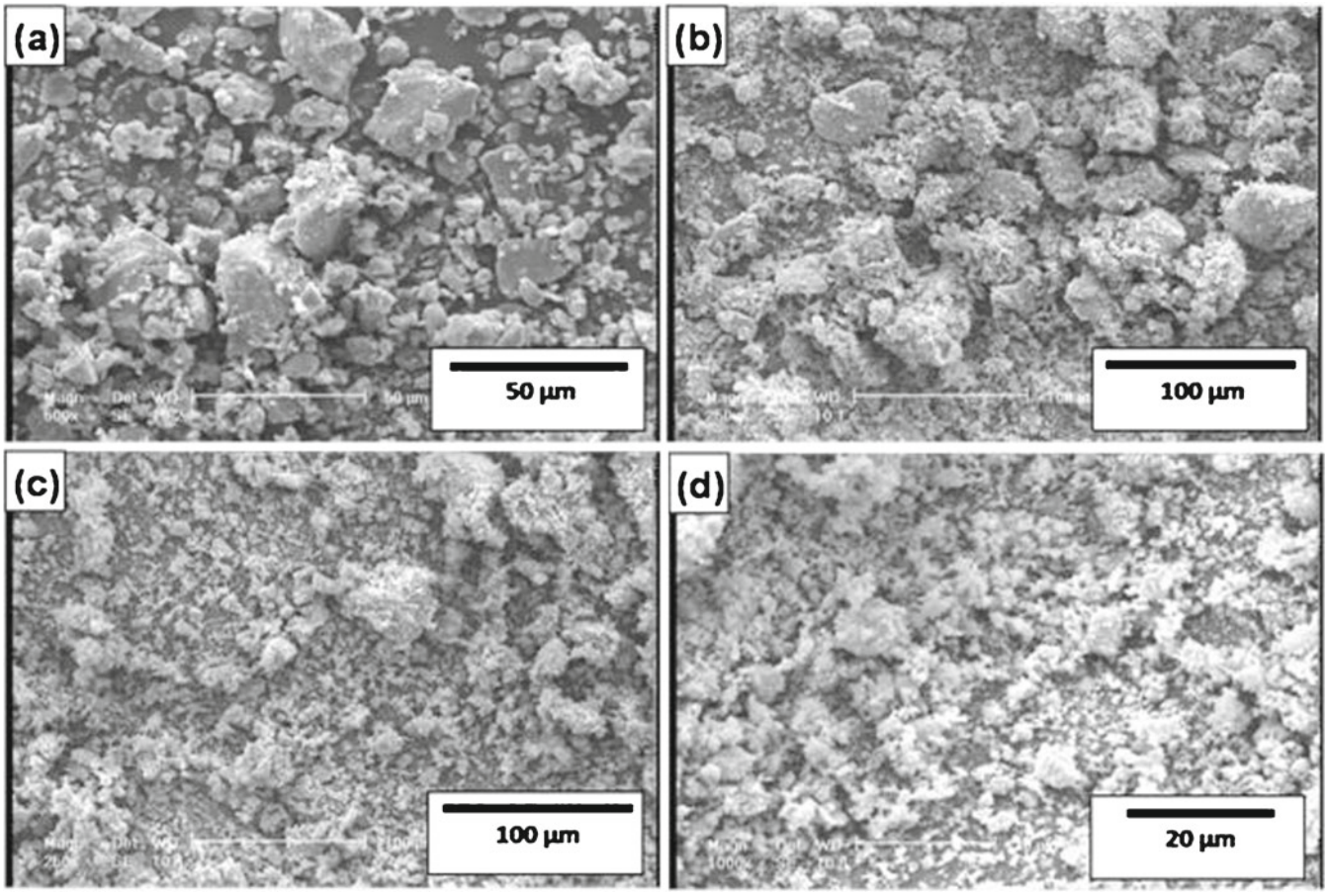

Figure 7. Morphology of $Ti_{62.5}Si_{37.5}$ powder mixture at different milling times: (**a**) 0·5 h, (**b**) 5 h, (**c**) 15 h and (**d**) 45 h.

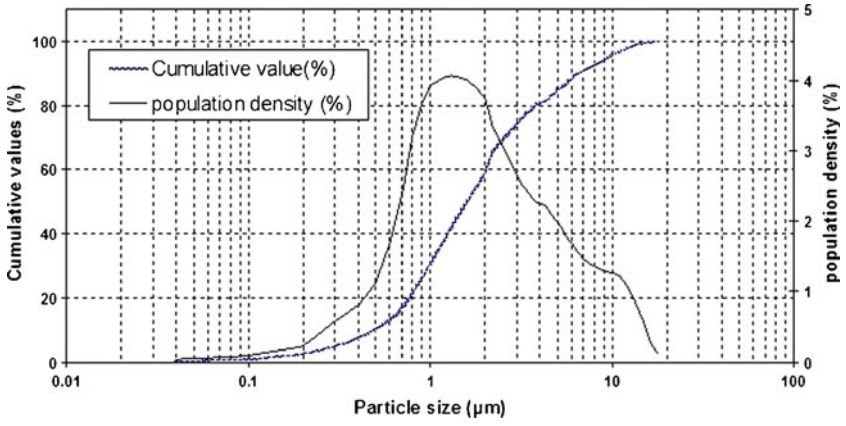

Figure 8. Particle size distribution of 45 h milled powders.

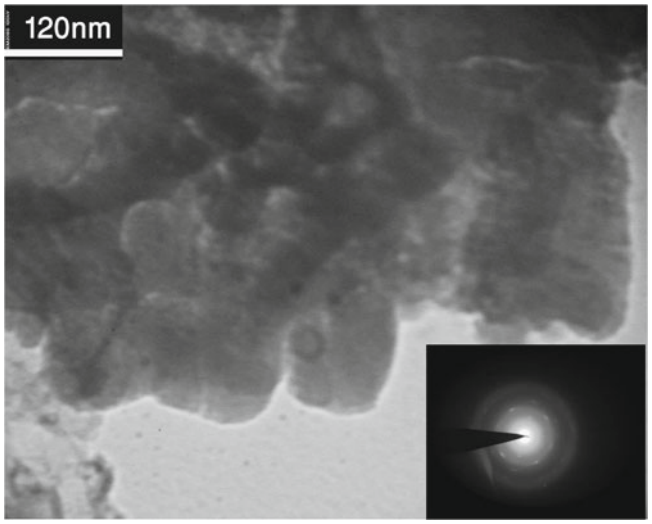

Figure 9. TEM image and selected area diffraction pattern of 60 h milled powders.

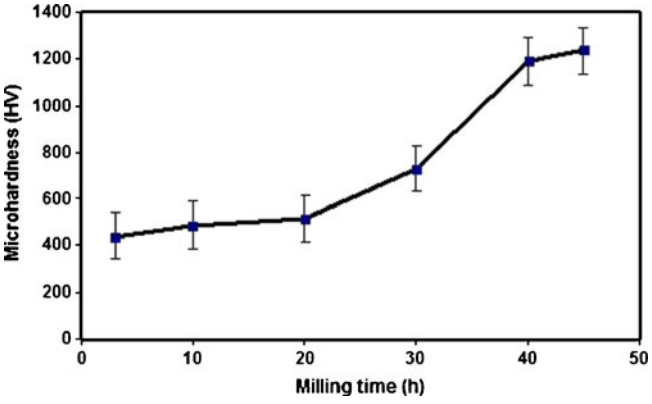

Figure 10. Microhardness values of mechanically alloyed $Ti_{62.5}Si_{37.5}$ powder mixture at different milling times.

welded particles between Si and Ti formed. Further milling to 15 h led to continuous decrease of powder particle size. After 45 h of milling time an agglomerated structure was formed due to the brittleness of Ti_5Si_3 intermetallic compound. In order to determine the mean particle size and size distribution of powders in this agglomerated structure (final powders), particle size analyser was used. Figure 8 shows particle size distribution of 45 h milled powders. As can be seen fine particles were formed with an average particle size of about 2·7 μm. Also it can be seen that all particles are <18 μm.

TEM image and related selected area diffraction pattern (SADP) of 60 h milled powders are shown in figure 9. TEM image clearly shows grains with <50 nm grain size. As can be seen, a relatively good agreement exists regarding the grain size of Ti_5Si_3 estimated from TEM observation and that of XRD analysis using Williamson–Hall method. The ring pattern of SADP also confirms fine crystallite size of 60 h milled powders.

3.2c *Microhardness measurements*: Figure 10 shows microhardness of powder particles after different milling times. As shown, increasing the milling time to 20 h caused a small increase in microhardness due to plastic deformation induced into powder particles and work hardening. After 20 h of milling, a considerable increase in microhardness was observed. This increase in microhardness value between 20 and 40 h of MA is due to the gradual formation of Ti_5Si_3 phase from the elemental components. Also after 40 h of milling, a low increase in microhardness was observed which is due to the decrease of crystallite size of Ti_5Si_3 intermetallic compound. Finally after 45 h of MA, microhardness of powders increased to 1235 HV which is a high value. Also the microhardness values of powder particles after annealing at 850 and 1050°C were achieved to be 1050 and 1000 HV, respectively (table 3). This noticeable decrease in hardness value is due to the grain growth, release of internal strain and phase transition during annealing. The high hardness value of Ti_5Si_3 intermetallic compound besides the high melting point and low density makes this material as structural material valuable for advanced aerospace applications and protective high temperature coatings.

4. Conclusions

Thermodynamic analysis using Miedema model showed that in the nominal composition of Ti_5Si_3 ($X_{Si} = 0{\cdot}375$), intermetallic phase has the lowest Gibbs free energy and is the stable phase compared to solid solution and amorphous phases. To evaluate the theoretical results, mechanical alloying of Ti and Si powders was carried out. Mechanical alloying of $Ti_{62.5}Si_{37.5}$ powder mixtures led to the synthesis of disordered nanocrystalline Ti_5Si_3 intermetallic phase in accordance with thermodynamic predictions. It was found that Ti_5Si_3 intermetallic compound forms via a continuous diffusive reaction of Ti and Si at layer interfaces. The crystallite size and microhardness values of Ti_5Si_3 after 45 h of MA reached about 15 nm and 1235 HV, respectively.

References

Bakker H, Zhou G F and Yang H 1995 *Prog. Mater. Sci.* **39** 159

Brands E A 1983 *Smithells metals reference book* (London: Butterworths) 6th ed.

Cullity B D 1978 *Elements of X-ray diffraction* (Menlo park, New York: Addison-Wesley) 2nd ed.

Cheon Y W, Jo Y J, Lee C M, Jang H S, Kim K B and Lee W H 2007 *Mater. Sci. Eng.* **A467** 89

Doppiu S, Monagheddu M, Cocco G, Maglia F, Anselmi-Tamburini U and Munir Z A 2001 *J. Mater. Res.* **16** 1266

Enayati M H, Karimzadeh F and Anvari S Z 2008 *J. Mater. Process. Technol.* **200** 312

Forouzanmehr N, Karimzadeh F and Enayati M H 2009 *J. Alloys Compd.* **471** 93

Guang R, Jing-En Z, Shemgqi X and Pengliang N 2006 *Mater. Sci. Eng.* **A416** 45

Kang B Y, Ryoo H S, Hwang W, Hwang S K and Kim S W 1999 *Mater. Sci. Eng.* **A270** 330
Kesheng Z, Shengqi X and Jing'en Zh 2007 *Mater. Sci. Eng.* **A445–446** 48
Li J, Jiang D and Tan Sh 2002 *J. Eur. Ceram. Soc.* **22** 551
Lu C J and Li Z Q 2005 *J. Alloys Compd.* **395** 88
Massalski T B and Okamoto H 1990 *Binary alloy phase diagram* (Materials Park, OH: ASM International) 2nd ed.
Miedema A R, DeBoer F R and Boom R 1981 *Physica* **B103** 67
Mousavi T, Karimzadeh F and Abbasi M H 2008 *Mater. Sci. Eng.* **A487** 46
Mousavi T, Abbasi M H and Karimzadeh F 2009 *Mater. Lett.* **63** 786
Niessen A K and Miedema A R 1983 *Bunsenges Ber. Phys. Chem.* **87** 717
Niessen A K, Miedema A R, De Boer F R and Boom R 1988 *Physica* **B151** 401
Oehring M and Bormann R 1991 *Mater. Sci. Eng.* **A134** 1330
Oleszak D, Burzynska-Szyszko M and Matyja H 1993 *J. Mater. Sci. Lett.* **12** 3
Rao K P and Zhou J B 2004 *J. Mater. Sci.* **39** 5471
Riley D P, Oliver C P and Kisi E H 2006 *Intermetallics* **14** 33
Suryanarayana C 2001 *J. Prog. Mater. Sci.* **46** 1
Takacs L 2002 *Prog. Mater. Sci.* **47** 355
Tang Z H, Williams J J, Tom A J and Akinc M 2008 *Intermetallics* **16** 1118
Thadhani N N, Namjoshi S, Counihan P J and Crawford A 1999 *J. Mater. Process. Technol.* **85** 74
Vander Kolk G J, Miedema A R and Niessen A K 1988 *J. Less-Common Met.* **145** 1
Wang H Y, Lu S J, Zha M, Li S T, Liu C and Jiang Q C 2008 *Mater. Chem. Phys.* **111** 463
Westbrook J H and Fleischer R L (eds) 2000 *Intermetallic compounds: Structural applications of intermetallic compounds* (UK: Wiley)
Williamson K and Hall W H 1953 *Acta Metall.* **1** 22
Yang J, Wu J and Hua W 2000 *Physica* **B279** 241
Yeh C L, Chen W H and Hsu C C 2007 *J. Alloys Compd.* **432** 90
Zhang L and Wu J 1998 *Acta Mater.* **46** 3535
Zhang Z J, Bai H Y, Qiu Q L, Yang T, Tao K and Liu B X 1993 *J. Appl. Phys.* **73** 1702